

A Comparative Study on Optimized Bias Current Density Performance of Cubic ZnB-GaN with Hexagonal 4H-SiC Based Impatts

Arnab Majumdar, Srimani Sen

Abstract—In this paper, a vivid simulated study has been made on 35 GHz Ka-band window frequency in order to judge and compare the DC and high frequency properties of cubic ZnB-GaN with the existing hexagonal 4H-SiC. A flat profile p^+pnn^+ DDR structure of impatt is chosen and is optimized at a particular bias current density with respect to efficiency and output power taking into consideration the effect of mobile space charge also. The simulated results obtained reveals the strong potentiality of impatts based on both cubic ZnB-GaN and hexagonal 4H-SiC. The DC-to-millimeter wave conversion efficiency for cubic ZnB-GaN impatt obtained is 50% with an estimated output power of 2.83 W at an optimized bias current density of 2.5×10^8 A/m². The conversion efficiency and estimated output power in case of hexagonal 4H-SiC impatt obtained is 22.34% and 40 W respectively at an optimum bias current density of 0.06×10^8 A/m².

Keywords—Cubic ZnB-GaN, hexagonal 4H-SiC, Double drift impatt diode, millimeter wave, optimized bias current density, wide band gap semiconductor.

I. INTRODUCTION

THE electromagnetic spectrum extending from 26.5–40 GHz and designated as Ka-band finds extensive applications in fields of satellite communication, radars in military aircrafts, space telescopes, etc. The Ka-band millimeter wave window frequency of 35 GHz exhibits relatively low attenuation leading to its wide popularity [1]. The advantages of millimeter wave system lies in reduction of antenna size with lighter weight, high accuracy and resolution and better signal penetration through cloud, smoke, dust, etc. The rain attenuation of radio waves is found to be significant in satellite communication at Ka-band [2], [3]. The propagation of wave through ionosphere plays a major role in the functioning of the most effective satellites [4]. Some Ka-band frequencies are utilised for vehicle speed detection. Kepler mission uses this frequency range to downlink the scientific data collected by space telescope [5]. Hence, innumerable and wide spread applications in fields of communication reveal that millimeter wave based technology is on the verge of significant growth. The solutions to this requirement are sources based on avalanche transit time diode established as its potential in form of high power generating source at microwave and millimeter wave and even at sub-millimeter wave frequency bands [6]. These diodes are used as

solid state transmitters in tracking radars, radiometers, missile seekers and in various civilian activities.

Impatt diodes cover electromagnetic spectrum from 30-300 GHz and even more. Impatts came out as premier solid state source capable of generating high frequency RF power. Impatts based on conventional materials like silicon, gallium arsenide, indium phosphide are most common at microwave and millimeter wave frequencies exhibiting sufficient output power [7]. However, materials with wide band gap like silicon carbide (SiC) and gallium nitride (GaN) can be used as an alternative base material replacing conventional materials for the development of impatts with more efficiency. Recent developments on various electronic and optoelectronic devices based on wide band gap materials are available in commercial semiconductor market [8]. The superior performance exhibited by these wide band gap devices can be assessed by considering Keyes' FOM and Johnson's FOM [9]. Unlike the Keyes' and Johnson's FOM for silicon being unity and that for gallium arsenide (GaAs) being 0.45 and 0.71 respectively, the same parameters for gallium nitride are 1.6 and 756 respectively while those for silicon carbide are 5.1 and 278 respectively. Thus, in comparison to traditional silicon and gallium arsenide, the wide band gap semiconductors exhibit much superior performance in terms of high frequency and high temperature.

SiC, a wide band gap semiconductor, crystallizes in numerous different polytypic forms; the important being 2H-SiC, 3C-SiC, 6H-SiC, 15R-SiC, etc. As a wide band gap semiconductor it has almost triple the band gap energy ($E_g = 2.2-3.25$ eV), almost three times higher breakdown electric field strength, almost four times higher thermal conductivity and two times higher electron saturation drift velocity as compared to Si [10]-[12]. Moreover, it is thermally and mechanically very stable and chemically inert. Owing to the above properties, SiC is an obvious choice as an excellent material for high temperature/high-voltage semiconductor electronics. It can be made as base materials for impatt to generate higher power and for higher frequency applications [13]. There is currently much interest in its use as a semiconductor material in the electronics where its high thermal conductivity, high electric field, breakdown strength and high maximum current density make it more promising than silicon for high powered devices [14]. Amongst the different polytypes, the availability and quality of single crystal wafers in 4H-SiC and 6H-SiC make these polytypes the most promising materials for electronics devices. Recent

Arnab Majumdar is with the Department of Metallurgical and Materials Engineering, National Institute of Technology, Durgapur, India (e-mail: xie.7802@gmail.com).

achievements in growth processing and characterization of 4H-SiC have enhanced their commercial availability [15]. With the advent of VLS growth technique, it is now possible to grow thick and controlled doped layers on 4H-SiC [16]. In recent years, scientists around the globe are carrying out continuous research activities on 4H-SiC based electronics devices. 4H-SiC based single drift Impatt exhibiting microwave oscillations have already been experimentally demonstrated at X-band [10]. Fabrication of 4H-SiC high-low SDR Impatt has already been carried out [11] yielding 1mW RF power at 7.75 GHz. Many more theoretical and experimental studies on Impatts based on 4H-SiC have recently been reported [17]-[19]. GaN ($E_g = 3.39$ eV at room temperature), on the other hand, is a binary III-V wide band gap semiconductor supporting peak internal electric field about five times higher than those of silicon and gallium arsenide, resulting in higher breakdown voltage and thus making it a suitable material choice for impatts handling high power, high voltage, high efficiency and high operating frequency. GaN is less noisy and chemically very stable at higher temperature. High quality GaN film can be grown on SiC substrate by MOCVD technique using a Si_xN_y inserting layer [20]. Thus, considerable progress in the growth of nitrides and in the light of maturity of fabrication technology and unique material properties, GaN appears to be one of the best choices for the development of semiconductor devices. GaN is seen to exhibit different polytype forms, viz., hexagonal Wurtzite GaN (Wz-GaN or α -GaN) and cubic Zinc Blende GaN (ZnB-GaN or β -GaN).

The authors in this paper have considered a symmetrically doped flat profile p^+pnn^+ double drift impatt diode based on cubic β -GaN and hexagonal 4H-SiC and have simulated at 35 GHz their DC and high frequency properties at optimized bias current density with respect to efficiency and output power taking into consideration the effects of mobile space charge. The simulated results presented in the paper will go a long way in helping the researchers to fabricate impatt diodes based on the mentioned wide band gap materials.

II. SIMULATION METHODOLOGY

A double drift p^+pnn^+ of Impatt is considered and simulated at Ka-band window frequency of 35 GHz. The transit time formula of Sze and Ryder [32] is used here for the design of doping profile. The highly doped substrates are p^+ and n^+ regions while n and p are epi-layers. The material parameters extracted from recent published papers [21]-[31] and Electronic Archive [33] are enlisted in Table I and the design parameters are enlisted in Table II. Fig. 1 depicts the doping profile and electric field profile of p^+pnn^+ DDR Impatt Diode.

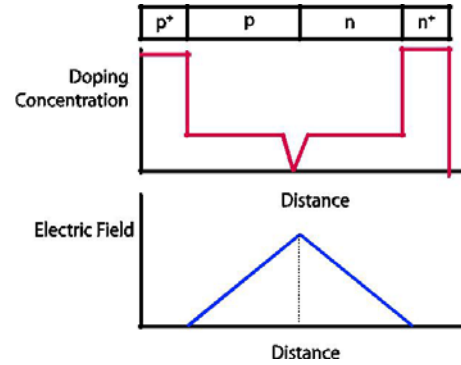


Fig. 1 Doping profile and Electric Field profile of p^+pnn^+ DDR Impatt Diode

The one dimensional model of the p-n junction is taken along with the electron and hole velocities being saturated and independent of the electric field throughout the space charge layer. The DC and small signal analysis of Impatts are carried out with the above stated assumptions. The DC electric field and carrier currents distribution in the depletion layer are obtained through double-iterative computer method. The electric field and carrier current profiles are obtained through computer simulation upon solving Poisson's equation, carrier continuity equations and space charge equation considering the effect of mobile space charge and carrier diffusion. The electric field at the depletion layer edges is subjected to the boundary condition

$$E(-x_1) = 0 \quad \text{and} \quad E(+x_2) = 0 \quad (1)$$

while the boundary conditions for the normalized current density $P(x) = (J_p - J_n)/J_0$ (where J_p = hole current density, J_n = electron current density) at the two edges are

$$P(-x_1) = (2/M_p - 1) \quad \text{and} \quad P(x_2) = (1 - 2/M_n) \quad (2)$$

where $-x_1$ and x_2 define the p^+ and n^+ edges of the depletion layer. The conversion efficiency is given by [34]

$$\eta(\%) = (1xV_d) / (\pi x V_B) \quad (3)$$

where V_d = Voltage drop across the drift region and V_B = Breakdown voltage. The breakdown voltage is obtained using

$$V_B = \int_{x_1}^{x_2} E(x) dx \quad (4)$$

where $-x_1$ = n-side depletion layer width and $+x_2$ = p-side depletion layer width.

The Gummel-Blue method [35] is used to find the range of frequencies exhibiting negative conductance of the diode. From the DC field and current profiles, the spatially dependent ionization rates that appear in the Gummel-Blue equations are evaluated, and fed as input data for the small signal analysis.

The diode impedance $Z(x, \omega)$ is splitted into real part $R(x, \omega)$ and imaginary part $X(x, \omega)$ [35] and a double-iterative modified Runge-Kutta method is used to solve the two equations simultaneously. The diode negative resistance ($-Z_R$) and reactance ($-Z_X$) are computed through numerical integration of $-R(x)$ and $-X(x)$ profiles over the active space-charge layer.

The negative conductance (G), Susceptance (B) and the quality factor (Q) of the device are calculated using:

$$-G = -Z_R / [(Z_R)^2 + (Z_X)^2]$$

$$B = Z_X / [(Z_R)^2 + (Z_X)^2]$$

$$-Q_{\text{peak}} = (B / -G) \text{ at peak frequency}$$

Here both $-G$ and B are normalized to the area of the diode. The maximum power output P_{RF} from the device at resonant frequency of oscillation is

$$P_{RF} = V_{RF}^2 (G_p) A/2 \quad (5)$$

where, V_{RF} is the amplitude of the RF swing ($V_{RF} \approx V_B/2$, assuming 50% modulation of V_B), G_p is the diode negative conductance at the operating frequency and A is the area of the diode ($=10^{-10} \text{ m}^2$).

TABLE I
MATERIAL PARAMETERS OF 4H-SiC AND ZnB-GaN

Material Parameters	4H-SiC	ZnB-GaN
Band gap Energy (eV)	3.26	3.2
Dielectric Constant	9.66	9.7
Critical Electric Field ($\times 10^7$ V/m)	0.37	20
Electron Mobility (m^2/Vs)	0.09	0.1
Saturated Electron Drift Velocity ($\times 10^5$ m/s)	2.2	2
Thermal conductivity (W/mK)	490	130
Ionization Coefficient of Electrons at Low fields, A_n (m^{-1})	4.57×10^{10}	1.023×10^9
Ionization Coefficient of Electrons at Low fields, b_n (m^{-1})	5.24×10^9	0.602×10^9
Ionization Coefficient of Holes at Low fields, A_p (m^{-1})	5.13×10^8	1.276×10^8
Ionization Coefficient of Holes at Low fields, b_p (V m^{-1})	1.57×10^9	0.376×10^9
Ionization Coefficient of Electrons at High fields, A_{hn} (m^{-1})	4.57×10^{10}	5.284×10^8
Ionization Coefficient of Electrons at High fields, B_{hn} (V/m)	5.24×10^9	0.547×10^9
Ionization Coefficient of Holes at High fields, A_{hp} (m^{-1})	5.13×10^8	8.328×10^7
Ionization Coefficient of Holes at High fields, B_{hp} (V/m)	1.57×10^9	0.323×10^9

TABLE II
DESIGN PARAMETERS OF 4H-SiC AND ZnB-GaN

Design Parameters	4H-SiC	ZnB-GaN
Width of n-epilayer W_n (μm)	2.3	0.3
Width of p-epilayer W_p (μm)	2.3	0.3
Total active layer width (μm)	4.6	0.6
Flat n-layer doping conc. ($\times 10^{23} \text{ m}^{-3}$)	0.68	2
Flat p-layer doping conc. ($\times 10^{23} \text{ m}^{-3}$)	0.68	2
Bias current density (A m^{-2})	0.06×10^8	3.2×10^9

TABLE III
DC AND SMALL SIGNAL PROPERTIES OF 4H-SiC AND ZnB-GaN

DC and small signals Properties	4H-SiC	ZnB-GaN
Breakdown Voltage (V)	783.92	84.1
Peak Frequency (GHz)	34.8	36
Efficiency (%)	22.34	15
Quality Factor	5.18	0.84
Estimated output power (W)	40.09	2.83
Peak Negative conductance (S m^{-2})	-5.22×10^6	-32×10^6

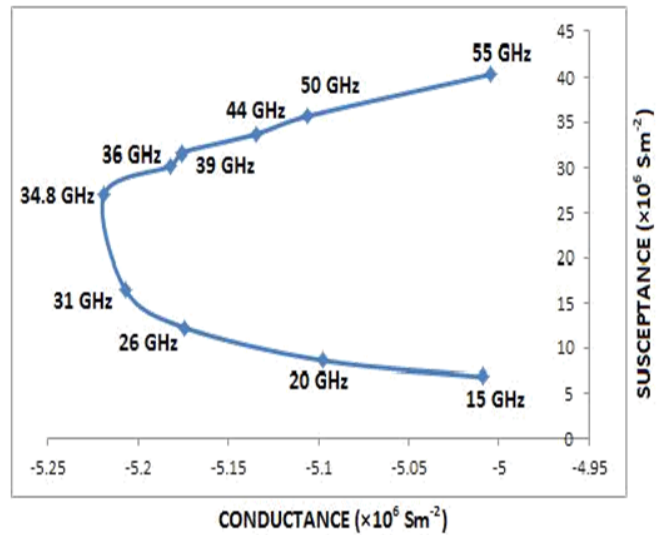


Fig. 2 The Conductance – Susceptance plot of cubic 4H-SiC DDR Impatt at 35 GHz and at an bias current density of $0.06 \times 10^8 \text{ A/m}^2$

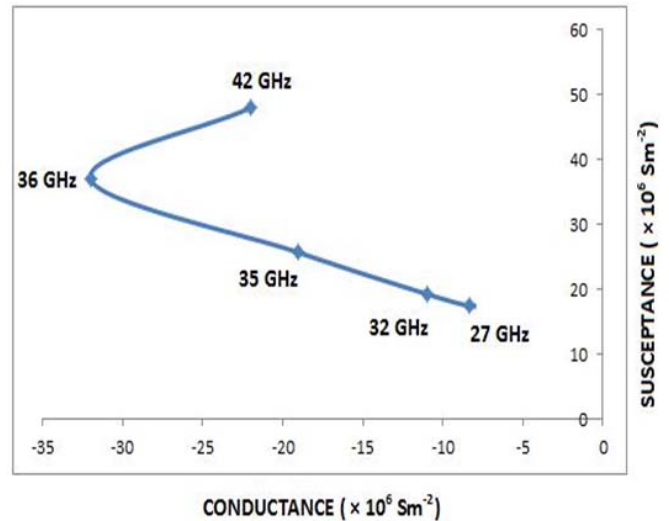


Fig. 3 The Conductance – Susceptance plot of cubic ZnB-GaN DDR Impatt at 35 GHz and at an bias current density of $3.2 \times 10^9 \text{ A/m}^2$

III. RESULTS AND DISCUSSIONS

The material parameters of 4H-SiC and ZnB-GaN are tabulated in Table I. The material parameters include band gap energy, dielectric constant, mobility, saturated drift velocity, critical electric field, thermal conductivity and ionization coefficient of electrons and holes at low and high fields. Table II depicts the structural or the design parameters for p^+pnn^+ flat

profile, linear impatt based on hexagonal 4H-SiC and cubic ZnB-GaN at Ka-band window frequency of 35 GHz. The width of both n and p-epilayers are taken to be same for the respective diodes with specific values of background doping concentration. As analytical methods do not provide accurate information, hence, computer simulation studies have been carried out to obtain the values of DC and small signal properties of the respective diodes. The simulated DC results which include DC field, current profiles and space dependent quantities are used to obtain the high frequency properties of the device which provides an insight into the mm-wave properties of the device. The simulation studies at different bias current densities have been carried out and the optimized bias current density results are presented in this paper. The DC and high frequency simulated results are enlisted in Table III. The optimized bias current density for 4H-SiC DDR Impatts is 0.06×10^8 A/m² and 3.2×10^9 A/m² for ZnB-GaN DDR Impatts. The breakdown voltage for 4H-SiC is 783.92 V and 84.1 V for ZnB-GaN. Thus, the wideband gap semiconductors based impatt exhibits a higher value for breakdown voltage and is thus expected to generate higher output power. The DC-to-millimeter wave conversion efficiency for 4H-SiC is 22.34% and 15% in case of ZnB-GaN Impatts.

The Q-factor determines the growth rate and stability of oscillation. Less Q-factor means better device performance. Here the Q-factor for impatts based on 4H-SiC and ZnB-GaN is 5.18 and 0.84 respectively. The real and imaginary parts of the diode admittance are computed for various bias current densities and for different frequencies to obtain conductance-susceptance (G-B) plot. The G-B plots for Impatts based on 4H-SiC and ZnB-GaN are shown in Figs. 2 and 3 respectively. The optimum frequency for peak negative conductance and the avalanche frequency at which G becomes negative are obtained from G-B plots. The peak negative conductance occurs at 34.8 GHz for 4H-SiC impatt which is very close to the design frequency of 35 GHz. The value for peak negative conductance in case of ZnB-GaN is found to occur at 36 GHz which is also very close to the design frequency of 35 GHz as is evident from the respective G-B plots. The value for peak negative conductance for 4H-SiC and ZnB-GaN Impatts is 5.22×10^6 S/m² and 32×10^6 S/m² respectively. The estimated output power at the design frequency of 35GHz and at respective optimum bias current density is 40.09 W and 2.83 W for 4H-SiC and ZnB-GaN based impatts respectively. Thus, the simulated results for DC and high frequency properties of the device as presented in the paper are very encouraging, promising and exhibits the strong potentiality and superior performance of impatts based on wide band gap semiconductors in terms of efficiency and output power.

IV. CONCLUSION

The simulated results presented in the paper shows that hexagonal 4H-silicon carbide DDR impatt generates high output power and high conversion efficiency at a particular optimum bias current density. The same results holds for impatts based on yet another wide band gap semiconductor namely cubic ZnB-GaN. Moreover, the peak negative

conductance for all these structures is very close to the design millimeter wave frequency of 35 GHz. Thus, it is possible to generate high output power at mm wave domain with the mentioned parameters facilitating the device fabrication process. The results presented will be very fruitful for the researchers worldwide to have a detail study on the subject.

REFERENCES

- [1] A.J. Gasiewski and M. Klein, —The Sensitivity of Millimeter and sub-millimeter frequencies to atmospheric temperature and water vapour variations, *Journal of Geophysical Research-Atmospheres*, 13, pp.17481-17511, 2000.
- [2] T.V. Omotosho and C.A. Oluwafemi, Impairment of Radio wave Signal by rainfall on fixed satellite service on Earth-Space path at 37 stations in Nigeria, *Journal of Atmospheric and Solar-Terrestrial Physics*, 71, pp. 830-840, 2009.
- [3] K. Nakazawa, S. Tanaka and K. Shogen, —A method to transform rainfall rate to rain attenuation and its application to 21GHz band satellite, *IEICE Trans. On Commun.*, E91-B(6), pp. 1806-1811, 2008.
- [4] S.K. Sarkar, —Some studies on attenuation and atmospheric water vapour measurement in India, *Int. J. Remote Sensing*, 19(3), 473-480, 1998.
- [5] Y. Maekawa, T. Fujiwara, Y. Shibagaki, T. Sato, M. Yamamoto, H. Hashiguchi and S. Fukao, —Effects of tropical rainfall to the K_u-band satellite communication links at the equatorial atmosphere RADAR observatory, *Journal of the Meteorological Society of Japan*, 84A, 211-225, 2006.
- [6] J.D. Gibson, Editor, *The Communication Handbook*, Second Edition, CRC Press, LCC.
- [7] R. Bauer, —Ka-band propagation measurement: An opportunity with Advanced Communications Technology Satellite (ACTS), *Proceedings IEEE*, 85, 853-862, 1997.
- [8] M. Shur —Terahertz Technology: Devices and Applications, *Proc. ESSDERC*, Grenoble, France, 2005.
- [9] V.V. Buniatyan and V.M. Aroutiounian, —Wide gap semiconductor microwave devices, *J. Phys. D, Appl. Physics*, 40(20), pp. 63555-6385, 2007.
- [10] K.V.Vassilevski, A.V.Zorenko and K.Zekentes, —Experimental observation of microwave oscillations produced by pulsed Silicon Carbide IMPATT diode, *ELECTRONICS LETTERS.*, Vol.37, No.7, pp. 466-467, 2001
- [11] L.Yuan, J.A.Cooper, Jr., K.J.Webb and M.R.Melloch, —Experimental demonstration of a silicon carbide impatt oscillator, *IEEE Electronic Devices Letters*, Vol. 22, No. 6, pp. 266-268, June 2001.
- [12] Konstantin Vassilevski, Alexander Zorenko, Konstantinos Zekentes, Katerina Tsagaraki, Edwige Bano, Christophe Banc and Alexander Lebedev, —4H-SiC IMPATT Diode Fabrication and Testing, pp. 713, 2001, *Technical Digest of International Conference on SiC and Related Materials – ICSRM2001*, Tsukuba, Japan, 2001.
- [13] Luo Yuan, James A. Cooper, Kevin J. Webb and Michael R. Melloch, —Demonstration of IMPATT Diodes Oscillators in 4H-SiC, *Technical Digest of International Conference on SiC and Related Materials – ICSRM 2001*, Tsukuba, Japan, 2001, pp. 723.
- [14] M. Bhatnagar and B.J. Baliya, —Comparison of 6H-SiC, 3C-SiC and Si for power devices, *IEEE Trans. On Electronic Devices*, Vol. 40, No. 3, pp. 645-655, March 1993.
- [15] R. Madar, —Silicon Carbide in contention, *Nature*, 430, pp. 1009-1012, 2006.
- [16] R. Yakimova and E. Janzen, —Current status in the growth of SiC, Diamond and Related materials, 9(3-6), pp. 432-438, 2000.
- [17] I.A. Khan and J.A. Cooper, —Measurement of high field electron transport in silicon carbide, *IEEE Trans. on Electronic Devices*, Vol. 47, No. 2, 2000.
- [18] S. Ono, M. Arai and C. Kimura, —Demonstration of High power X-band oscillation in p⁺nn⁺ 4H-SiC impatt diodes with guard ring termination, *Materials Science Forum*, 981-4, pp. 483-485, 2005.
- [19] J. H. Zhao, Monte Carlo simulation of 4H-SiC impatt diode, *Semicond. Sci. & Technol.*, 15, pp. 1093-1100, 2000.
- [20] K.J.Lee, Growth of High quality GaN epilayers with Si_xN_y inserting layer on Si <111> substrate, *Journal of the Korean Physical Society*, Vol-45., pp-S756-S759, 2004.
- [21] Soumen Banerjee, Riya Chkrabarti and Riya Baidya, —Bias current

- optimization study on avalanche transit time diode based on Wurtzite and ZnB phase of GaN at THz frequency, *Int. J. of Advanced Science & Technology*, 28, 35-44, 2011.
- [22] Soumen Banerjee, —Dynamic characteristics of IMPATT diodes based on wide band gap and narrow band gap semiconductors at W-band, *Int. J. of Engineering Science & Technology*, 3(3), 2149-2159, 2011.
- [23] M.Mukherjee, Soumen Banerjee and J.P. Banerjee, —Dynamic characteristics of III-V and IV-IV semiconductor based transit time device in the THz range regime: A comparative analysis, *Int. J. of Terahertz Science and Technology*, 3(3), 97-109, 2010.
- [24] M.Mukherjee, Nilratan Majumdar and S.K. Roy, —Photosensitivity analysis of GaN and SiC Terahertz IMPATT Oscillator: Comparison of theoretical reliability and study on experimental feasibility. *IEEE Trans. On Device and Material Reliability*, 3(8), 608-620, 2008.
- [25] A.K. Panda, D. Pavlidis and E. Alekscev, —DC and high frequency char. of GaN based IMPATTs, *IEEE Trans. on Electron Devices*, 4(48), 2001.
- [26] A.K. Panda, D. Pavlidis and E. Alekscev, —Noise characteristics of GaN based IMPATTs, *IEEE Trans. on Electron Devices*, 7(48), 2001.
- [27] Soumen Banerjee, Priya Chakrabarti and Riya Baidya, —Effect of bump width on the efficiency of high-low 4H-SiC impatt at Ka-band window frequency, *Int. Journal of engineering science and technology*, Vol. 2, Issue 10, pp. 5657-5661, October 2010.
- [28] M.Mukherjee, Soumen Banerjee and J.P. Banerjee, — MM-wave performance of DDR impatts based on cubic SiC, *Proc. of XVth International Workshop on the Physics of Semiconductor Devices (IWPSD)*, pp. 533-536, SSPL & Jamia Millia Islamia, New Delhi, 2009.
- [29] M. Mukherjee, —Prospects of α -SiC and β -SiC based p^+pnn^+ impatt devices as sub-mm wave high power sources, *Proc. of International Conference on Microwave*, pp. 34-37, Jaipur, India, 2008.
- [30] Soumen Banerjee and J.P. Banerjee, —Effect of punch through factor on the breakdown characteristics of 4H-SiC impatt diode, *Proc. of IEEE-MTTs International Conference on Recent Advances in Microwave theory and Applications (Microwave-08)*, pp. 59-62, 2008, Jaipur, India.
- [31] S. Mukhopadhyay, Soumen Banerjee, J. Mukhopadhyay and J.P. Banerjee, —Mobile Space charge effect in 4H-SiC impatt diode, *Proc. of XIVth International Workshop on the Physics of Semiconductor Devices (IWPSD)*, TIFR & IIT Bombay, pp. 268-272, Mumbai, India, 2007.
- [32] S.M. Sze and R.M. Ryder, —Microwave Avalanche diodes, *Proc. IEEE, Special Issue on Microwave Semiconductor Devices*, 1971.
- [33] Electronic Archive: <http://www.ioffe.ru/SBA/NSM/Semicond/GaN>.
- [34] L. Scherfetter and H.K. Gummel, —Large signal analysis of a silicon read diode oscillator, *IEEE Trans. on Electron Devices*, 1(6), 1969.
- [35] H.K. Gummel and J.L. Blue, —A small signal theory of Avalanche Noise in IMPATT Diodes, *IEEE Trans. on Electron Devices*, 14, 562, 1967.

Arnab Majumdar, student of National Institute of Technology, Durgapur, pursuing B.Tech course in Metallurgical and Materials Engineering for the session of 2014-2018. He has his schooling from Narendrapur Ramakrishna Mission Vidyalaya with a state rank of 20 in +2 level (WBCHSE). He also has three published paper publications in IEEE on Secured Routing Protocols in October, 2015.